ACS APPLIED MATERIALS & INTERFACES

Research Article

Cite This: ACS Appl. Mater. Interfaces 2018, 10, 43252−43261

www.acsami.org

Adhesion between Hydrophobic Elastomer and Hydrogel through Hydrophilic Modification and Interfacial Segregation

Kevin Tian,[†] Jinhye Bae,[†] Zhigang Suo,*[,†,‡] and Joost J. Vlassak*[,†]

[†]Harvard School of Engineering and Applied Sciences and [‡]Kavli Institute for Bionano Science and Technology, Harvard University, Cambridge, Massachusetts 02138, United States

Supporting Information

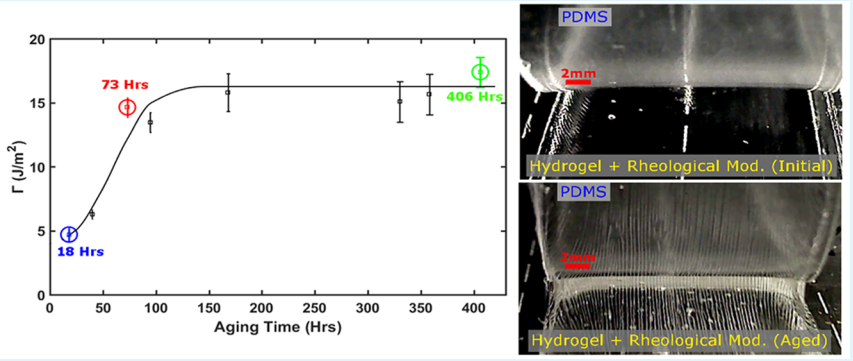

ABSTRACT: Recent progress in the printing of soft materials has made it possible to fabricate soft stretchable devices for a range of engineering applications. These devices tend to be heterogeneous systems, and their reliability depends to a large extent on the integrity of the interfaces between the various materials in the system. Previous studies on the printing of hydrogels have highlighted the need to investigate the adhesion between extrusion printable dielectric elastomers and hydrogels. Here we consider polydimethylsiloxane (PDMS) and a polyacrylamide hydrogel that contains lithium chloride and a nonionic rheological modifier. We show that the adhesion between oxygen plasma-treated PDMS and the hydrogel increases with time to reach a stable value of 15 J m^{-2} after ∼6 days. During that time, the contact angle of water on the PDMS interface remains constant at ∼30°, suggesting that hydrophobic recovery of plasma-treated PDMS is suppressed by the presence of the hydrogel. It is further observed that a thin viscous layer develops at the interface between PDMS and hydrogel, which results in energy dissipation upon debonding and which allows full recovery of the adhesion after debonding and rejoining. This viscous layer develops only in the presence of the rheological modifier in the hydrogel and the hydrophilic surface treatment of the PDMS.

KEYWORDS: *PDMS, hydrogel, hydrophobic recovery, extrusion printable hydrogel, ionic conductor, adhesion, self-healing interface*

INTRODUCTION

Soft materials have recently risen in popularity for a wide variety of engineering applications, particularly in the areas of soft robotics,[1,2] stretchable electronics,[3,4] and biomedical devices.[5−7] Most designs require the integration of dissimilar soft materials into a single device. For instance, ionic devices have seen several suites of functionalities developed from combinations of hydrogels and elastomers.[8−12] These devices illustrate the materials' dissimilarity as a functional necessity: a hydrogel serves as an electrical conductor and a hydrophobic elastomer serves as a dielectric. As these devices become more sophisticated, more care must be given to their manufacture. Although great progress has been made in the extrusion-based fabrication of stretchable electronic[3,4] and ionic[13−15] devices, less attention has been devoted to a more subtle but equally important problem: how reliable are these manufacturing techniques for dissimilar materials? In this context, the interfacial adhesion is critical to the reliability of a broad range of materials, including composites,[16,17] dental adhesives,[18] and biological organisms.[19,20] Recent forays into soft-materials extrusion printing have acknowledged adhesion as important but have rarely quantified the adhesion between dissimilar materials within printed systems.[13,15] As devices become more sophisticated and complex, crack driving forces may easily scale such that delamination becomes a serious problem. Neither predictive capability nor process optimization is possible without quantification of adhesion. Therefore, as manufacturing processes are adapted for soft materials, studies that quantify the adhesion between dissimilar materials must be conducted.

One area of manufacturing that has seen particularly rapid development is 3D extrusion printing, as research has expanded the materials roster from thermoplastics to include metals,[21] ceramics,[22] and soft materials such as hydrogels and

Received: September 20, 2018
Accepted: November 21, 2018
Published: November 21, 2018

DOI: 10.1021/acsami.8b16445
ACS Appl. Mater. Interfaces 2018, 10, 43252−43261

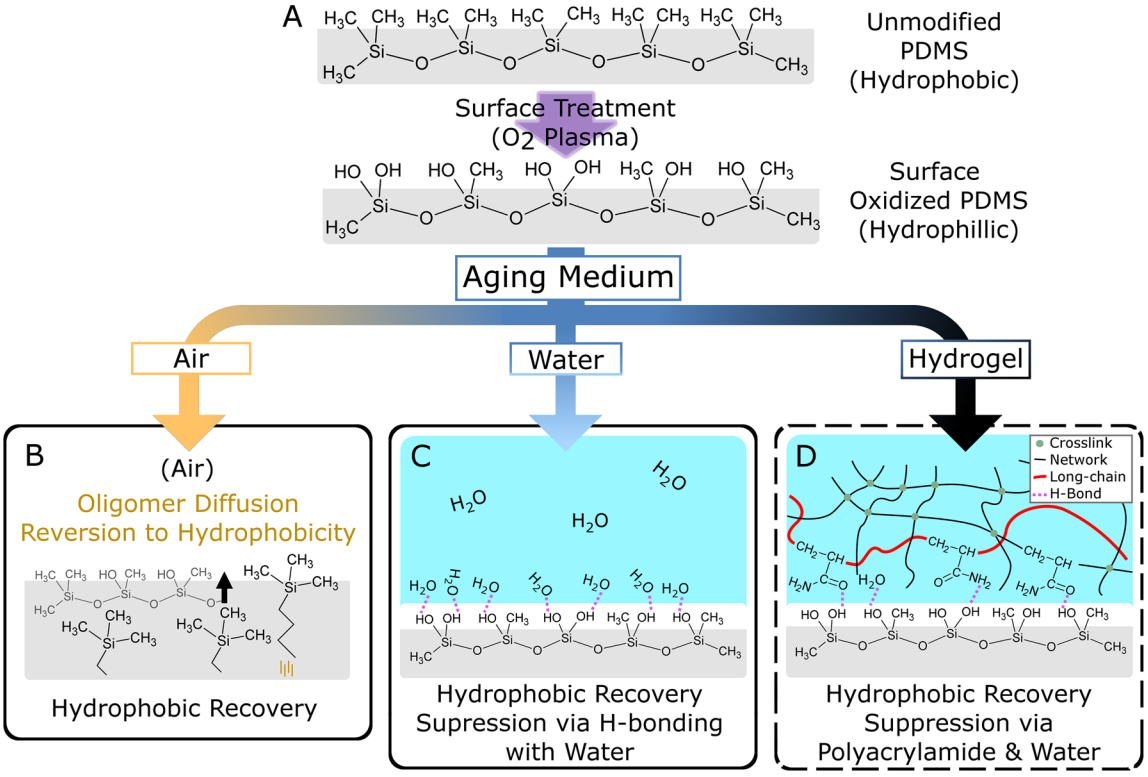

Figure 1. (A) Illustration of the change in surface chemistry of a PDMS sample upon exposure to an oxidizing surface treatment. (B–D) Illustration of the possible fates for a surface oxidized PDMS sample, where the surface silanol groups are either (B) dominated by hydrophobic recovery while exposed to the atmosphere or (C) hydrogen bonded with a polar solvent and suppress hydrophobic recovery. (D) This work proposes an alternative method of preserving the hydrophilic surface of PDMS through direct contact with a hydrogel, which also enables the preservation of the interfacial adhesion between hydrogel and PDMS.

elastomers.[6,7,13,15,23−25] In our previous work, we identified hygroscopic-salt-containing polyacrylamide (PAAm) hydrogel and polydimethylsiloxane (PDMS) as suitable materials that can be integrated in an extrusion printing process for ionic devices.[15] The hygroscopic salt served to maintain water content while enhancing electrical conductivity.[26] The fabrication process developed utilized rheological tuning combined with surface energy matching of PDMS via plasma oxidation to allow for consistent submillimeter extrusion printing of a hydrogel precursor onto PDMS. Controlling the rheological behavior of the precursor is essential to achieving 3D extrusion printable hydrogels;[27] an established method for this is by adding a rheological modifier to the hydrogel precursor such as un-cross-linked PAAm,[7,13,15] alginate,[24] or synthetic clay.[23] As part of the fabrication procedure, the PAAm hydrogel precursor contained a PAAm-based rheological modifier to tune its extrusion behavior. Incidentally, the use of un-cross-linked PAAm chains as a rheological modifier enables the printed hydrogels to be optically transparent, which is significant to some devices.[11,12] To ensure good wetting of the PDMS by the hydrogel precursor, the PDMS surface was treated with oxygen plasma. However, since PDMS plasma-based surface treatments are known to be transient,[28−32] the long-term stability of the adhesion between a hydrogel and PDMS remains in question. As these materials are common within stretchable electronics/ionics, the adhesive interactions at the interface of hydrogel and hydrophobic elastomer are of broad interest.

The general strategy of plasma oxidation treatments for improving adhesion and wetting is well established for a wide variety of materials, including polycarbonate,[33] oxides,[4] glass,[34] and silicon wafers.[35] When PDMS is exposed to an oxygen plasma, surface methyl groups are converted into silanol groups[31,34] (Figure 1A). The silanol groups are capable of hydrogen bonding with water and thus render the surface of the plasma-oxidized PDMS hydrophilic.

However, PDMS also exhibits a hydrophobic recovery of its surface chemistry that is almost always dominated by the migration of residual siloxane oligomers toward the surface.[29−31,36−38] If exposed to the atmosphere, plasma-oxidized PDMS reverts back to a hydrophobic state in a matter of hours[29,36,39,40] (Figure 1B). A similar instability of plasma-based surface treatments is observed in other materials, although the time scale of recovery is extremely material dependent.[33,41] Even though methods exist for mitigating hydrophobic recovery, such as thermal aging,[29] solvent extraction,[32] and chemical grafting,[28] these processes are generally incompatible with 3D extrusion. This would suggest that within the context of extrusion printing the interfacial adhesion between hydrogel and plasma-treated polymer may degrade due to hydrophobic recovery.

On the other hand, the absence of delamination in fatigue tests in our previous work suggests that the PDMS/hydrogel interface may be stable.[15] Because suppression of hydrophobic recovery has been observed with PDMS in contact with an aqueous medium[42,43] (Figure 1C), we hypothesize that the water in the hydrogel suppresses hydrophobic recovery through formation of hydrogen bonds with the silanol groups in the PDMS surface (Figure 1D). A hydrophilic surface, by definition, physically binds with water in an energetically

DOI: 10.1021/acsami.8b16445
ACS Appl. Mater. Interfaces 2018, 10, 43252−43261

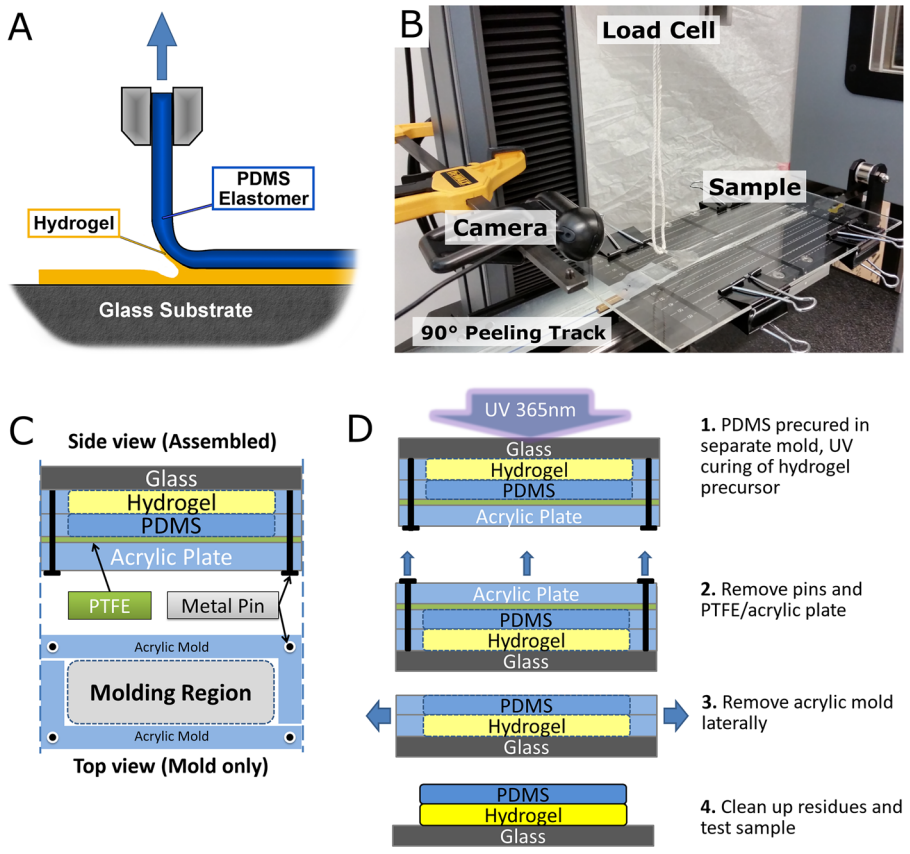

Figure 2. (A) Illustration and (B) photograph of the experimental setup for adhesion measurements using a 90° peeling setup. (C) A schematic overview of the segmented mold developed to preserve sample interface integrity. (D) The sequence of sample fabrication, assuming a fully assembled mold stack.

favorable manner and thus must contain polar functional groups with which water may interact. It is therefore reasonable that such a surface would also bind with other polar groups and improve the adhesion with another material. For instance, silanol groups on a plasma-treated PDMS surface could form hydrogen bonds with polar groups in a hydrogel network, enhancing the adhesion between both materials. The presence of water molecules and polar groups at the interface would also reduce the driving force for the diffusion of hydrophobic species in the PDMS to the interface and impede hydrophobic recovery. We therefore posit that the hydrogen-bonding interaction includes polar species such as water as well as the acryloyl and amide functional groups present in both the hydrogel network and the rheological modifier. This mechanism establishes the possibility that hydrogels are capable of stabilizing the adhesion with plasma-treated PDMS, with possible extensions to other polymers or elastomers. Therefore, the aim of this paper is to quantify the adhesion between plasma-treated PDMS and hydrogel over an extended period of time.

Interfacial adhesion has been characterized by a wide variety of methods,[44] including angled peeling,[45] lap shear,[46] scratch,[47] and flexure[48,49] testing. The applicability of these methods to very soft materials capable of large deformations is, however, not well established. For instance, peeling tests have problems with hysteresis due to bending induced plasticity in the samples, while most other tests are either invalid beyond small-strain assumptions or ill-suited for soft materials.[48] Even so, there exist several techniques that are suitable for evaluating the adhesion of hydogels, including bilayer shear-based tests[50] and 90° peeling tests.[3,4] We selected the 90° peeling test (Figure 2A,B) because it is both compatible with the samples of interest and because it is a simple and standardized method for which adhesion energies are readily compared.

This study reports on the stability of the interfacial adhesion in materials systems that consist of printable hydrogels and PDMS. During this investigation, we were able to verify the long-term reliability of the adhesion but also observed segregation of a viscous phase to the interface, which had a significant impact on the adhesive behavior. We demonstrate that this segregation is directly related to the surface treatment of the PDMS and the presence of the rheological modifier in the hydrogel precursor. This finding suggests that long-chain polymer additives, which were originally added to tailor the viscosity of the hydrogel precursor, also aid in the long-term reliability of the PDMS/hydrogel interface and possibly of other materials systems.

RESULTS AND DISCUSSION

Sample Preparation and Processing. The hydrogel precursor formulation as described by Tian et al.[15] contains lithium chloride (LiCl) salt and un-cross-linked PAAm. The materials used in this study were chemically identical to those used by Tian et al.,[15] but the samples were cast instead of printed. To facilitate the casting process, the viscosity of the hydrogel precursor was decreased by reducing the amount of rheological modifier to 36.7% of the network polymer (see the Experimental Section for exact weight percentages). This

DOI: 10.1021/acsami.8b16445
ACS Appl. Mater. Interfaces 2018, 10, 43252−43261

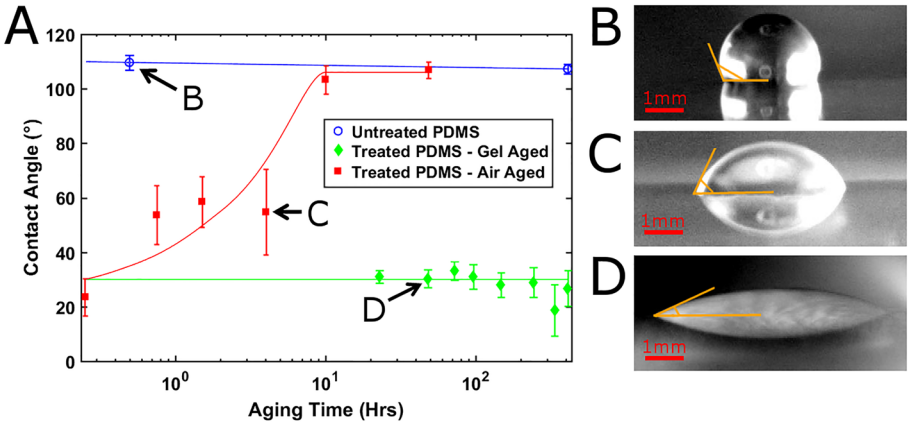

Figure 3. (A) Contact angle measurements over a period of 400 h of untreated PDMS and plasma-treated PDMS aged in contact with hydrogel (green diamond) or exposed to atmosphere (red square), with all lines to act as a guide to the eye; samples were all stored under RH control of 47%. Images illustrating (B) hydrophobic (at 109.9°), (C) weakly hydrophilic (at 54.8°), and (D) hydrophilic (at 30.3°) regions of the behavior are shown.

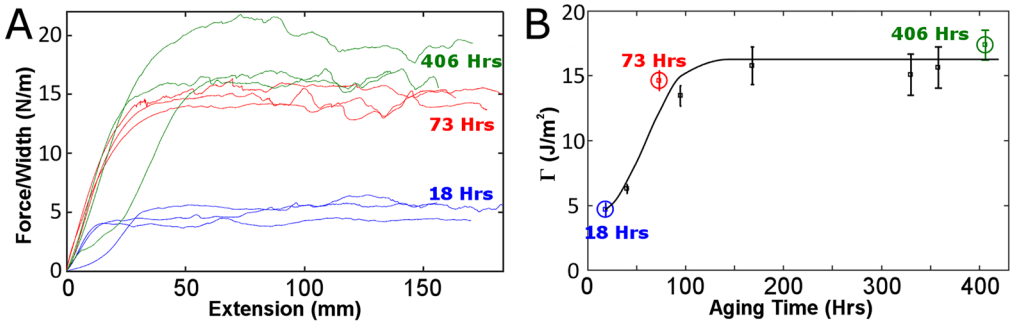

Figure 4. (A) An example of the hydrogel−elastomer bilayer interfacial peeling data used to calculate the plateau peeling force, presented as a plot of peeling force divided by sample width against peeling extension. (B) A plot of the interfacial toughness of the plasma-treated PDMS and PAAm hydrogel interface observed over a 408 h time period, with black line as a guide to the eye. Highlighted in blue, red, and green are data points at 18, 73, and 406 h represented by the peeling data illustrated in (A).

amount of modifier still yields a rheology that is suitable for extrusion printing (Figure S1), although with reduced resolution. The modification in the hydrogel formulation was driven by the need to fabricate macroscopic samples in a reasonable amount of time so that a statistically significant number of samples could be tested with peeling forces that were large enough to be measured accurately with available load cells. The interfacial adhesion of the cast samples and the underlying mechanisms are not expected to differ significantly from samples that were printed beyond potential effects of shear deformation during extrusion. This shear could cause some degree of polymer alignment, which, if we use the rubbing shear-alignment of polystyrene (PS) as a proxy, may slightly reduce adhesion.[51] This alignment may also result in some anisotropy in the interfacial toughness, which is not considered in this study.

Samples were fabricated using a split mold that allowed removal of the samples from the mold without applying any forces perpendicular to the bilayer interface (Figure 2C,D). This procedure was used for all samples, even though it was strictly only necessary for samples with very weak adhesion. Once the hydrogel precursor and PDMS were cured in contact, samples were aged in a controlled environment with 42% relative humidity between 18 and 408 h. The environmental control during aging was necessary to ensure that the swelling ratio of hydrogel would not change during aging. A 90° peel test setup was then used to measure the adhesive energy of the hydrogel−PDMS bilayers, whereby the PDMS was peeled off from the hydrogel layer affixed to a glass substrate (Figure 2A). Data from the 90° peel tests consisted of peeling force against peeling extension. All tests were initiated by making a precrack of <5 mm and were performed at a constant peeling rate of 50 mm/min for a length of at least 100 mm. After the crack began to propagate through the bilayer, the peeling force eventually settled into a steady-state regime. The expression for the strain energy release rate during peeling[52] is $G = \frac{F}{b}(1 - \cos\theta)$ for peel angle θ, peel force F, and sample width b. For 90° peeling, this expression simplifies to $G = \frac{F}{b}$. Under steady-state crack propagation, the interfacial fracture energy Γ is equal to G, so that Γ is given by the plateau peeling force divided by the width of the specimen.

Hydrophobic Recovery and Interfacial Adhesion. The contact angles of water on various PDMS surfaces are shown in Figure 3A as a function of aging time. The contact angle on untreated PDMS was initially measured to be $\theta = 109.9 \pm 2.8°$ (Figure 3B), consistent with the extreme hydrophobicity of untreated PDMS, and remained unchanged during aging. A plasma-treated PDMS surface that was aged under atmospheric conditions only retained its hydrophilicity for a short period of time (Figure 3C) and reverted to a hydrophobic state within 10 h. The behavior of untreated and treated PDMS during aging matches that reported in the literature[31,53,54] and is thus not particularly remarkable. On the other hand, plasma-treated

DOI: 10.1021/acsami.8b16445
ACS Appl. Mater. Interfaces 2018, 10, 43252−43261

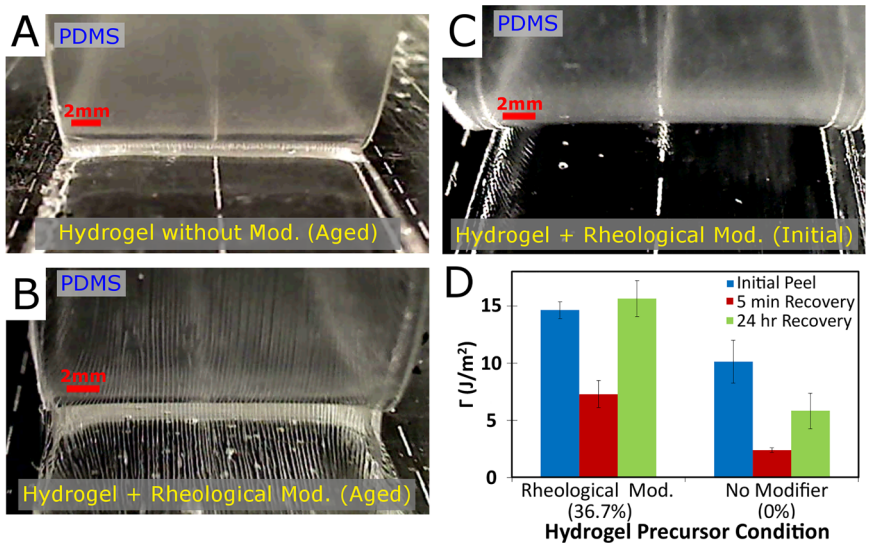

Figure 5. (A) A representative image of a peeling test after 336 h of aging for a hydrogel containing no rheological modifier cured in contact with oxygen plasma-treated PDMS. (B, C) These representative images illustrate peeling tests of PDMS off hydrogels containing rheological modifier at aging time of 73 and 18 h, respectively. (D) Plot of the adhesion recovery at different waiting times, 5 min and 24 h, of the plasma-treated PDMS–hydrogel interface for hydrogels both with and without the rheological modifier.

PDMS surfaces aged in contact with a hydrogel were able to retain their hydrophilicity, $\theta \sim 30°$, for a period of at least 408 h, although the average values of the contact angle were slightly higher than the initial contact angle of treated PDMS, $\theta = 23.5 \pm 6.9°$. This result suggests that there is an interaction between the hydrogel and the silanol groups on the PDMS surface that suppresses hydrophobic recovery. The graph shows clearly that even a brief exposure to the atmosphere degrades the contact angle on treated PDMS. It is now necessary to relate these changes in contact angle relate to interfacial adhesion before any conclusion can be drawn.

Figure 4 shows the results of the peel tests as a function of interface aging time. As illustrated in the figure, the measured adhesion energy changes significantly with aging: it increases from an initial value of $\Gamma = 4.69 \pm 0.53$ J m^{-2} to $\Gamma = 14.63 \pm 0.75$ J m^{-2} after 73 h, i.e., a 3-fold enhancement in adhesion. Although this behavior is not explained by any mechanism based on the hydrophobic recovery hypothesis, it is clear that the adhesion is stable at its plateau value of 15 J m^{-2} for up to 408 h after the initial aging period. If hydrophobic recovery had occurred during aging, the adhesion would have degraded due to the reduction in physical bonding between hydrogel and elastomer or a reversion of the contact angle of the PDMS surface back to a hydrophobic state. Because neither of these effects were observed, the surface treatment must be preserved, verifying the hypothesis that hydrophobic recovery of plasma-treated PDMS is inhibited by the presence of a hydrogel. This new form of hydrophobic recovery suppression may be useful for preserving the surface treatments of PDMS and polymers in general, both within the context of printed soft materials and beyond.

Viscous Dissipation at the Hydrogel–Elastomer Interface. During adhesion testing, a viscous fingering instability developed at the interface between the hydrogel and the PDMS. In controlling for the rheological modifier (Figure 5A,B), it became apparent that this phenomenon is directly related to the presence of the rheological modifier in the hydrogel. A hydrogel without any rheological modifier was cast and aged for a period of 336 h, but no fingering was observed (Figure 5A), while a hydrogel with modifier showed extensive fingering after ~73 h (Figure 5B,C). With aging, a viscous layer develops at the hydrogel–PDMS interface leading to fingering during delamination. We believe that energy dissipation in this viscous layer contributes to the interfacial adhesion, consistent with models of the adhesive failure of viscoelastic solids,[55] and is in fact the reason why the adhesion improves with aging. The only other time-dependent phenomenon expected in this context is hydrophobic recovery of the PDMS, which is readily ruled out since this mechanism would lead to a decline in adhesion. Visually, the phenomenon appears similar to the fingering instabilities first observed in the study of viscoelastic adhesion.[56] They have also been observed in elastic systems,[57] such as when peeling rigid plates from elastic adhesive films[58] and the elastic instabilities present during the peeling of pressure-sensitive adhesives.[59] That these instabilities remain after peeling suggests that the material responsible for the fingering is extremely viscous, which is indeed the case for the rheological modifier.

The viscous layer leaves a visible residue on the PDMS surface, as well as filaments on the hydrogel surface, indicating that the interfacial fracture propagates within the viscous layer rather than at the interface of hydrogel or PDMS. A consequence of this viscous residue is that it allows for completely reversible adhesion between the hydrogel and PDMS, as illustrated in Figure 5D. The figure shows a simple experiment in which a hydrogel–PDMS bilayer was first aged for at least 96 h to ensure full development of the viscous layer, then delaminated and readhered without additional applied pressure (i.e., only gravity), and finally delaminated again after the specified amount of time. At each delamination step the adhesion energy was measured. The observation is that the adhesion in the final delamination recovers 107 ± 11% of its previous value after 24 h if the hydrogel has the rheological modifier, but only 57 ± 33% without the modifier. We believe that the reduced adhesion in the latter case is due to partial hydrophobic recovery. When the plasma-treated PDMS surface is exposed to the atmosphere for ~10 min after delamination, it undergoes hydrophobic recovery. This does

DOI: 10.1021/acsami.8b16445
ACS Appl. Mater. Interfaces 2018, 10, 43252–43261

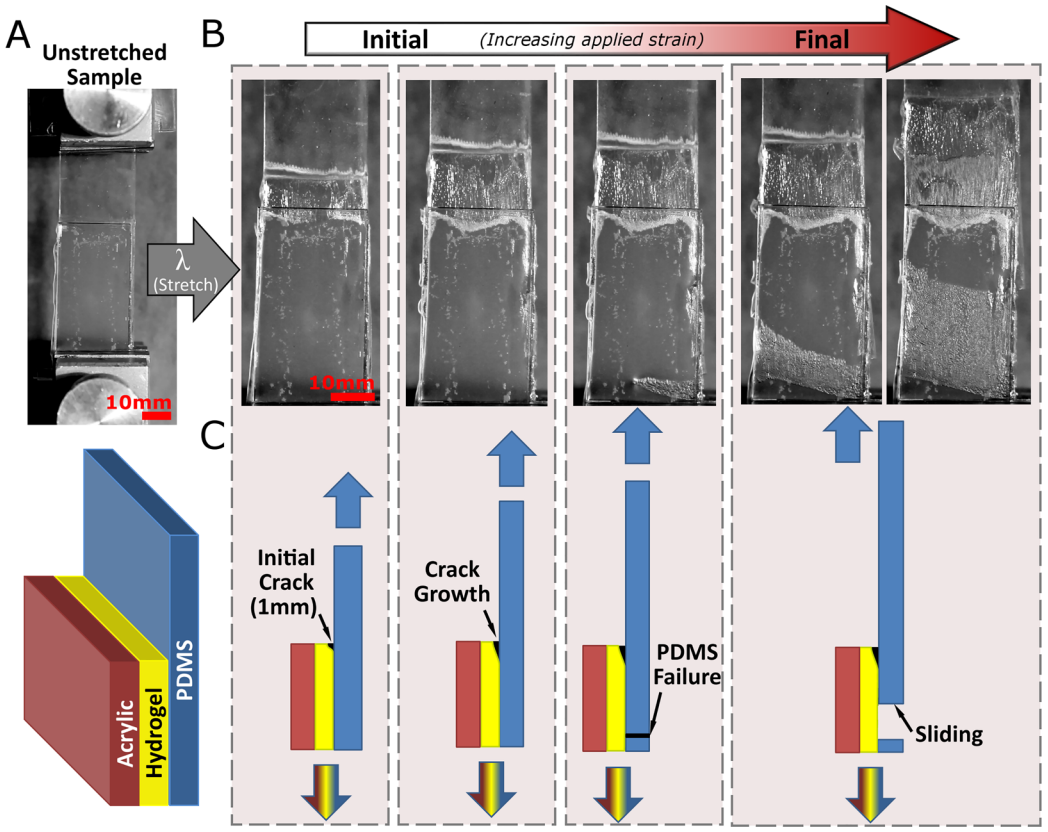

Figure 6. Bilayer shear testing performed on an aged hydrogel−PDMS interface. Photos have been decolorized for clarity. (A) shows the sample and a representative schematic of the unstretched sample (schematic not to scale). Acrylic, hydrogel, and PDMS layers had thicknesses of 1.6, 0.5, and 1.6 mm, respectively; all had a width of 25 mm. (B) As the sample is stretched at a rate of 10 mm/min, the PDMS portion is deformed while the thinner hydrogel layer, bonded to a stiff acrylic plate, is constrained. With increased strain the PDMS eventually fails and displays a slide/relaxation phenomenon that is readily explained by the presence of a viscous layer at the hydrogel−PDMS interface. (C) An equivalent schematic representation of the previously described sample as it is stretched.

not happen for the samples with the rheological modifier because the viscous residue that is left on the surface of the PDMS acts as a medium with which silanol groups in the PDMS can form hydrogen bonds. The adhesion is then dominated by the dissipation that the viscous layer affords; i.e., the viscous layer acts as a pressure-sensitive adhesive binding the bilayer together.

Because the viscous layer significantly alters the behavior of the interface when loaded under mainly mode I conditions, we also evaluated the effect of the viscous layer when the interface is loaded mainly in shear. We thus conducted a mode II dominated delamination test to evaluate whether the failure mode was different from previously observed hydrogel−elastomeric bilayer systems[50] (Figure 6A). As Figure 6B illustrates, the crack front only propagates a small distance despite the stiff backing layer applied to the hydrogel to drive the bilayer toward delamination. Instead of steady-state crack propagation, the PDMS substrate fails and proceeds to slide across the hydrogel surface; this can be inferred from the lack of apparent flow or motion in the central region where the fractured PDMS and hydrogel remain in contact. There is a significant amount of viscous residue remaining on both hydrogel and PDMS, as observed in the 90° peel tests. The critical energy release rate, G, for this geometry can be determined using the method described by Tang et al.[50] and is approximately $G = 29.88\ \mathrm{J\ m^{-2}}$ shortly prior to substrate failure (see Figure S2 for hydrogel viscoelastic moduli). We note that the crack front of the sample propagated a small amount but then stopped even after the PDMS substrate failed and began sliding back (Figure 6B and Video S1). This behavior is due to the flowing of the viscous layer as the sample is deformed in shear (Figure 6C). Contrary to the mode I scenario where the two materials are separated perpendicularly, in mode II the materials are kept in contact with the viscous layer at all times.

Several possibilities were considered regarding the origin of the viscous layer. For instance, the viscous layer could be the result of incomplete curing caused by the presence of oxygen in the PDMS given the high gas permeability of the material.[28,60] However, the lack of viscous fingering in a hydrogel cured without rheological modifier suggests otherwise (Figure 5A). Separate combinations of hydrogel−PDMS curing tests showed that viscous fingering occurred only when both the PDMS was plasma-treated and the rheological modifier was present in the hydrogel. Both hydrogels with and without rheological modifier were found to have negligible adhesion and no viscous fingering after peeling from untreated PDMS. Furthermore, it was impossible to reproduce the effect even after 350 h of aging if the rheologically modified hydrogel was cured separately and subsequently placed in contact with plasma-treated PDMS. These observations suggest that the hydrogel must be cured in contact with the treated PDMS surface to reproduce the segregation. Because the un-cross-linked PAAm used as rheological modifier has a high molecular weight and is quite viscous, this requirement may arise from

DOI: 10.1021/acsami.8b16445
ACS Appl. Mater. Interfaces 2018, 10, 43252−43261

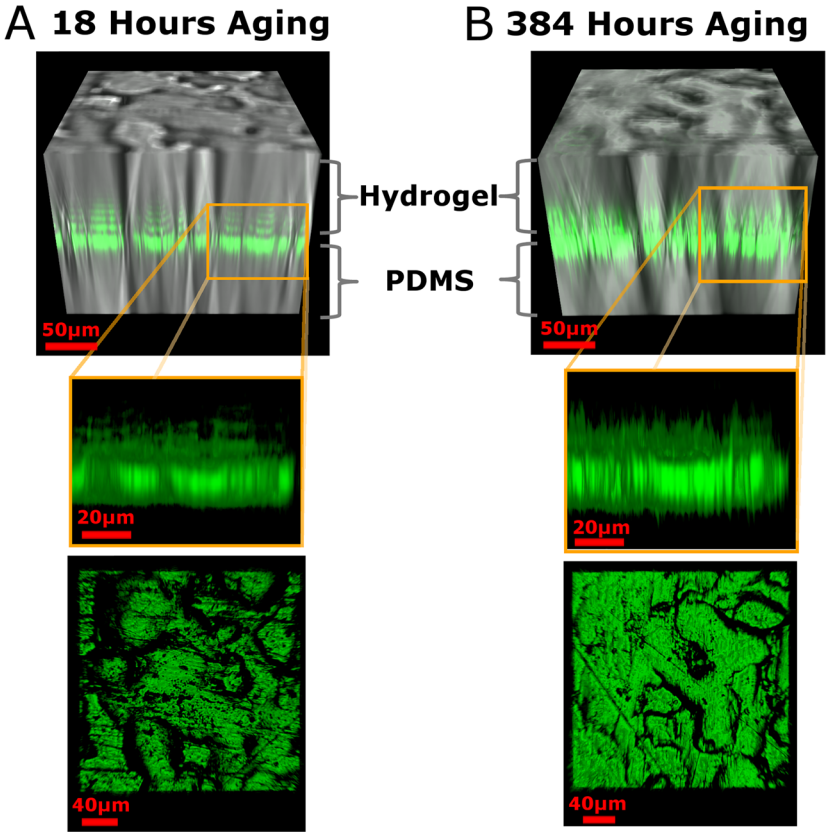

Figure 7. Fluorescence confocal imaging of the PDMS−hydrogel interface, having containing tagged the un-cross-linked PAAm chains with fluoroscein *o*-acrylate and aged for (A) 18 h or (B) 384 h. 3D reconstruction utilized scans centered on the interface ±100 μm and included both bright field and fluorescence channels for the perspective view; top and side views of the reconstruction used only the fluorescence channel.

the difficulty of the PAAm chains diffusing to the surface in the presence of a fully formed network. We further note that hydrogen bonding as a driving force acts equally on both the hydrogel network and the rheological modifier, given that they are chemically indistinguishable aside from the low-density cross-links, but only the rheological modifier is mobile. Because hydrogen bonding is typically a short-range driving force, we suggest that a fraction of the rheological modifier can migrate to the PDMS interface pregelation, which partially anchors these chains to the interface via hydrogen bonding. Once anchored, these polymer chains may continue their migration to the interface postgelation through a pull-out process.

The segregation phenomenon was further confirmed by means of fluorescence confocal microscopy using fluorescently tagged un-cross-linked PAAm chains as rheological modifier. Figure 7 makes it abundantly clear that the PAAm chains are in fact aggregating as a macroscopic, ∼30 μm thick layer at the interface between the hydrogel and PDMS and that this layer is present as early as 18 h after sample fabrication. As the bilayer is aged beyond 18 h, we observe that (1) the thickness of the layer continues to increase from an initial 30 to 50 μm and (2) visible levels of un-cross-linked PAAm remain within the hydrogel network. This result strongly suggests that this phenomenon is indeed a bulk-to-interface segregation of the rheological modifier within the PAAm hydrogel. Although recent studies have described how bulk-to-interface viscous flows can contribute to hydrogel adhesion,[61] there are no previous reports of fluids in hydrogels undergoing macroscopic phase separation from bulk to interface. Furthermore, the observation that no segregation occurs if the hydrogel is cured separately from the treated PDMS suggests the need for an initial "seed layer" at the interface that forms during the network curing stage and that allows continued segregation after the hydrogel is fully cured. That this layer continues to grow in thickness at a slow rate could be explained as a diffusion-driven process,[62] whereby the un-cross-linked polymer chains are drawn from the network to the interface; however, it is difficult to establish whether this is due to chain anchoring or some other driving force in the system. The adhesion enhancement that comes with the migration of the viscous layer must arise from the entanglement that is inevitable for long polymer chains contained within a cross-linked network. This entanglement allows viscous dissipation at the interface, greatly enhancing the adhesion. The fact that significant amounts of residue remain on the PDMS surface signifies that the hydrogen bonds between the viscous layer and the PDMS are not readily severed, making the situation a viscoelastic analogue to the classical tethered polymer melt at the interface between two polymers.[63] The introduction of this rheological modifier changes the nature of the adhesion from simple physical bonding into one where polymer chains are pulled out of their entangled state, albeit one where the chains are not chemically anchored to either surface.[63,64]

CONCLUSIONS

Evaluation of the interfacial adhesion as well as contact angle measurements demonstrates that a hydrogel is capable of stabilizing PDMS surface oxidation treatments for extended periods of time while in direct contact. Furthermore, we have

DOI: 10.1021/acsami.8b16445
ACS Appl. Mater. Interfaces 2018, 10, 43252−43261

discovered that a macroscopic viscous layer segregates to the interface of a hydrogel−PDMS system if the hydrogel precursor contains a long-chain rheological modifier and the PDMS surface has been plasma treated with oxygen. This viscous layer enhances adhesion by increasing energy dissipation during delamination, a picture that is consistent with accepted models for interfacial failure in adhesives[55] and earlier studies on adhesion enhancement through viscous dissipation.[65−67] The presence of the viscous layer also results in fully reversible interfacial adhesion. This result highlights a simple method for improving the fabrication by printing of integrated systems of soft materials using preexisting techniques and materials that are readily available. Because the surface modification strategy employed here is applicable to polymers in general, the combination of rheological modifiers and plasma treatments may be an effective method for improving the adhesion for any printed heterogeneous material system consisting of a hydrogel and an elastomer.

EXPERIMENTAL SECTION

Preparation of PDMS. Sylgard 184 (Dow Corning) was mixed at the prescribed 10:1 ratio and cast into a 20 mm × 200 mm × 1.6 mm acrylic mold, followed by degassing for 1 h at 70 kPa vacuum. The degassed PDMS was then sealed by applying pressure with another acrylic plate and cured in an oven at 65 °C for 24 h. The PDMS either is used immediately following removal from the mold or undergoes further surface treatment. Prior to surface treatment, the PDMS was rinsed with DI water and isopropyl alcohol and then dried with nitrogen. The PDMS is then treated with oxygen plasma (SPI Supplies, Plasma Prep II) at an O_2 pressure of 18 psi, vacuum chamber pressure of 275 mTorr, and RF power of 80 W for 60 s. After treatment, the PDMS is immediately placed in DI water for transport and dried with N_2 prior to use.

Preparation of Hydrogel. The PDMS segments are placed within a segmented acrylic mold to allow for hydrogel precursor to be cast directly onto the PDMS surface and cured while in direct contact; the mold may then be separated horizontally and removed such that the PDMS−hydrogel interface is maintained (Figure 2A,B). The hydrogel precursor consisted of acrylamide (AAm, Sigma-Aldrich, A8887), α-ketoglutaric acid (α-keto, Sigma-Aldrich), *N*,*N*,*N*′,*N*′-tetramethylethylenediamine (TEMED, Sigma-Aldrich, T7024), *N*,*N*′-methylenebis(acrylamide) (MBAA, Sigma-Aldrich, 146072), and lithium chloride (LiCl, Sigma-Aldrich, 746460) dissolved in either DI water or a polyacrylamide (PAAm) solution. Mixing was performed using a planetary centrifugal mixer (Thinky, ThinkyMixer ARE-300). The PAAm solution was synthesized by UV exposing a solution containing AAm, α-keto, and TEMED at a dose rate of 1.2 mW/cm^2 at 365 nm for 18 h at 25 °C. The PAAm solution precursor used a mass ratio of 94.23% deionized water (resistivity = 18.2 MΩ cm), 5.60% AAm, 0.1203% α-keto, and 0.05311% TEMED. The hydrogel precursor final mass ratios were 63.37% DI water, 3.623% PAAm, 9.88% AAm, 23.036% LiCl, 0.02635% MBAA, 0.0461% α-keto, and 0.0171% TEMED. In the cases where no rheological modifier was introduced, the precursor used the mass ratios: 66.12% DI water, 9.54% AAm, 24.25% LiCl, 0.02774% MBAA, 0.0485% α-keto, and 0.0180% TEMED. All hydrogel precursors were exposed to a 15 W bench UV lamp (XX-15, UVP) at a distance of 1 cm, yielding an average dose rate of 30 mW/cm^2 at 365 nm for 45 min. Samples for the bilayer shear debonding test were made using the same methods, but with the additional step of adhering the hydrogel to an acrylic sheet using a thin layer of cyanoacrylate adhesive (Krazy Glue).

Contact Angle Measurement. Measurements were made using a commercial contact angle measurement system (First Ten Angstroms, FTA135) to assist with image capture. Images were then manually processed to obtain the contact angle. Each measurement utilized a single 10 μL drop of DI water on a previously untested sample surface and was performed after a delay of 20 s to allow wetting to stabilize. Untreated PDMS was used as a control and a treated PDMS surface was either exposed to atmosphere or made contact with a hydrogel using the segmented mold method described in the "Preparation of Hydrogel" section. All samples were stored under a relative humidity of 47%. Because of residue from the hydrogel, PDMS samples kept in contact with a hydrogel were rinsed under DI water for 30 s and dried under N_2 for 30 s prior to contact angle measurements. At least five measurements were made for each condition, and all measurements for the same condition were made within a single 5 min interval.

Mechanical Characterizations. Peeling tests were performed on a dual column mechanical tester (Instron, 5966), with 10 N load cell (Instron, 2530-428) and 90° peel test fixture (Instron, 2820-035) at a constant displacement rate of 50 mm min^{-1}. The PDMS portion of the sample was peeled off the hydrogel, with the latter physically attached to a glass substrate during curing. Because the PDMS formulation used in this study is relatively stiff with a Young's modulus of 1−3 MPa,[68] a backing layer for the PDMS was not necessary to prevent excessive strains under load. All samples were fabricated to be 1.6 mm × 20 mm × 200 mm per material layer and stacked to form a 3.2 mm thick bilayer. A 2 mm hole was punched into one end of the PDMS to allow for cotton twine to be fed through and thus extend the distance between sample and load cell to minimize the effect of misalignment. Samples were first aligned and then a small initial crack (2 mm) at the front of sample was made. Peeling was then performed for the remainder of the sample, and the interfacial adhesion energy, Γ, was extracted from the steady-state region of the peeling force. Tensile testing of bulk hydrogel samples used the same mechanical test frame with a 500 N load cell (Instron, 2530-500N). Samples for this condition were cast into acrylic molds with a dog-bone geometry (Figure S4). All samples were tested with a 1500 mm min^{-1} displacement rate, were deformed to 300% stretch (150 mm), and held for 5 min (Figure S5). Bilayer shear-debonding tests were completed on a mechanical testframe (Instron, 3342 Single Column UTS) with a 50 N load cell (Instron, 2519-50N) at a displacement rate of 10 mm min^{-1}.

Confocal Imaging. Fluorescence confocal imaging was used to track the distribution of the rheological modifier within the hydrogel−PDMS bilayer. Imaging was performed on a confocal microscope (Leica Microsystem, TCS SP5) with a 10× dry objective and an argon laser excitation at 488 nm. Image acquisitions of 258 μm × 258 μm were made along the *z*-axis in 1 μm steps. ImageJ software was used in the 3D reconstruction of the imaging data. The fluorescently tagged un-cross-linked PAAm solution was prepared by making a separate instance of the PAAm solution precursor that substituted 10 wt % of the AAm with 10 wt % of fluorescein *o*-acrylate (FOA, Sigma-Aldrich, 568856) and resulted in FOA copolymerized within the PAAm chains. This tagged-PAAm was mixed with untagged PAAm solution at a ratio of 1:9, and the resulting solution was integrated with the hydrogel precursor as described previously in the "Preparation of Hydrogel" section. All other sample preparation steps were otherwise identical.

ASSOCIATED CONTENT

Supporting Information

The Supporting Information is available free of charge on the ACS Publications website at DOI: 10.1021/acsami.8b16445.

Video S1 (MPG)
Video S2 (AVI)
Video S3 (MPG)
Figures S1−S5 pertaining to rheological modifier data and sample geometry (PDF)

AUTHOR INFORMATION

Corresponding Authors

*(J.J.V.) E-mail: vlassak@seas.harvard.edu.
*(Z.S.) E-mail: suo@seas.harvard.edu.

DOI: 10.1021/acsami.8b16445
ACS Appl. Mater. Interfaces 2018, 10, 43252−43261

ORCID

Kevin Tian: 0000-0003-4821-4959

Zhigang Suo: 0000-0002-4068-4844

Author Contributions

K.T. and J.B. contributed equally to this work. The study was jointly designed by K.T., J.B., Z.S., and J.J.V. and executed by K.T. and J.B.

Funding

This research was supported by NSF (CMMI-1404653) and by the Harvard University MRSEC via NSF (DMR-1420570). Part of this work was performed at facilities supported by NSF (ECS 1541959).

Notes

The authors declare no competing financial interest.

■ ACKNOWLEDGMENTS

The authors also acknowledge Canhui Yang and Qihan Liu for fruitful discussions and intellectual contributions to this work. This research was supported with funding from the National Science Foundation under Grant CMMI-1404653 and by the Harvard University MRSEC, which is funded by the National Science Foundation under Grant DMR-1420570. Part of this work was performed at the Center for Nanoscale Systems (CNS), which is supported by the National Science Foundation under Grant ECS 1541959.

■ ABBREVIATIONS

PDMS, polydimethylsiloxane; AAm, acrylamide; PAAm, polyacrylamide; PTFE, polytetrafluoroethylene; LiCl, lithium chloride; RH, relative humidity.

■ REFERENCES

(1) Kern, M. D.; Ortega Alcaide, J.; Rentschler, M. E. Soft Material Adhesion Characterization for in Vivo Locomotion of Robotic Capsule Endoscopes: Experimental and Modeling Results. *J. Mech. Behav. Biomed. Mater.* **2014**, *39*, 257−269.

(2) Menguc, Y.; Park, Y.; Martinez-Villalpando, E.; Aubin, P.; Zisook, M.; Stirling, L.; Wood, R. J.; Walsh, C. J. Soft Wearable Motion Sensing Suit for Lower Limb Biomechanics Measurements. In *2013 IEEE International Conference on Robotics and Automation*; IEEE: 2013; pp 5309−5316.

(3) Yuk, H.; Zhang, T.; Parada, G. A.; Liu, X.; Zhao, X. Skin-Inspired Hydrogel-Elastomer Hybrids with Robust Interfaces and Functional Microstructures. *Nat. Commun.* **2016**, *7*, 12028.

(4) Lin, S.; Yuk, H.; Zhang, T.; Parada, G. A.; Koo, H.; Yu, C.; Zhao, X. Stretchable Hydrogel Electronics and Devices. *Adv. Mater.* **2016**, *28*, 4497.

(5) Muth, J. T.; Vogt, D. M.; Truby, R. L.; Mengüç, Y.; Kolesky, D. B.; Wood, R. J.; Lewis, J. A. Embedded 3D Printing of Strain Sensors within Highly Stretchable Elastomers. *Adv. Mater.* **2014**, *26* (36), 6307−6312.

(6) Hanson Shepherd, J. N.; Parker, S. T.; Shepherd, R. F.; Gillette, M. U.; Lewis, J. A.; Nuzzo, R. G. 3D Microperiodic Hydrogel Scaffolds for Robust Neuronal Cultures. *Adv. Funct. Mater.* **2011**, *21* (1), 47−54.

(7) Barry, R. A.; Shepherd, R. F.; Hanson, J. N.; Nuzzo, R. G.; Wiltzius, P.; Lewis, J. A. Direct-Write Assembly of 3D Hydrogel Scaffolds for Guided Cell Growth. *Adv. Mater.* **2009**, *21* (23), 2407−2410.

(8) Sun, J.-Y.; Keplinger, C.; Whitesides, G. M.; Suo, Z. Ionic Skin. *Adv. Mater.* **2014**, *26* (45), 7608−7614.

(9) Yang, C. H.; Chen, B.; Zhou, J.; Chen, Y. M.; Suo, Z. Electroluminescence of Giant Stretchability. *Adv. Mater.* **2016**, *28* (22), 4480−4484.

(10) Yang, C. H.; Chen, B.; Lu, J. J.; Yang, J. H.; Zhou, J.; Chen, Y. M.; Suo, Z. Ionic Cable. *Extrem. Mech. Lett.* **2015**, *3*, 59−65.

(11) Keplinger, C.; Sun, J.-Y. J.-Y.; Foo, C. C.; Rothemund, P.; Whitesides, G. M.; Suo, Z. Stretchable, Transparent, Ionic Conductors. *Science* **2013**, *341* (6149), 984−987.

(12) Yang, C.; Suo, Z. Hydrogel Ionotronics. *Nat. Rev. Mater.* **2018**, *3* (6), 125−142.

(13) Robinson, S. S.; O'Brien, K. W.; Zhao, H.; Peele, B. N.; Larson, C. M.; Mac Murray, B. C.; van Meerbeek, I. M.; Dunham, S. N.; Shepherd, R. F. Integrated Soft Sensors and Elastomeric Actuators for Tactile Machines with Kinesthetic Sense. *Extrem. Mech. Lett.* **2015**, *5*, 47−53.

(14) Larson, C.; Peele, B.; Li, S.; Robinson, S.; Totaro, M.; Beccai, L.; Mazzolai, B.; Shepherd, R. Highly Stretchable Electroluminescent Skin for Optical Signaling and Tactile Sensing. *Science* **2016**, *351* (6277), 1071−1074.

(15) Tian, K.; Bae, J.; Bakarich, S. E.; Yang, C.; Gately, R. D.; Spinks, G. M.; in het Panhuis, M.; Suo, Z.; Vlassak, J. J. 3D Printing of Transparent and Conductive Heterogeneous Hydrogel-Elastomer Systems. *Adv. Mater.* **2017**, *29*, 1604827.

(16) Teixeira de Freitas, S.; Sinke, J. Test Method to Assess Interface Adhesion in Composite Bonding. *Appl. Adhes. Sci.* **2015**, *3* (1), 1−13.

(17) Herrera-Franco, P. J. J.; Drzal, L. T. T. Comparison of Methods for the Measurement of Fibre/Matrix Adhesion in Composites. *Composites* **1992**, *23* (1), 2−27.

(18) Marshall, S. J.; Bayne, S. C.; Baier, R.; Tomsia, A. P.; Marshall, G. W. A Review of Adhesion Science. *Dent. Mater.* **2010**, *26* (2), e11−e16.

(19) Pesika, N. S.; Tian, Y.; Zhao, B.; Rosenberg, K.; Zeng, H.; McGuiggan, P.; Autumn, K.; Israelachvili, J. N. Peel-Zone Model of Tape Peeling Based on the Gecko Adhesive System. *J. Adhes.* **2007**, *83* (4), 383−401.

(20) Lee, B. P.; Messersmith, P. B.; Israelachvili, J. N.; Waite, J. H. Mussel-Inspired Adhesives and Coatings. *Annu. Rev. Mater. Res.* **2011**, *41*, 99−132.

(21) Skylar-Scott, M. A.; Gunasekaran, S.; Lewis, J. A. Laser-Assisted Direct Ink Writing of Planar and 3D Metal Architectures. *Proc. Natl. Acad. Sci. U. S. A.* **2016**, *113* (22), 6137−6142.

(22) Grida, I.; Evans, J. R. G. Extrusion Freeforming of Ceramics through Fine Nozzles. *J. Eur. Ceram. Soc.* **2003**, *23* (5), 629−635.

(23) Hong, S.; Sycks, D.; Chan, H. F.; Lin, S.; Lopez, G. P.; Guilak, F.; Leong, K. W.; Zhao, X. 3D Printing of Highly Stretchable and Tough Hydrogels into Complex, Cellularized Structures. *Adv. Mater.* **2015**, *27* (27), 4035−4040.

(24) Bakarich, S. E.; in het Panhuis, M.; Beirne, S.; Wallace, G. G.; Spinks, G. M. Extrusion Printing of Ionic−covalent Entanglement Hydrogels with High Toughness. *J. Mater. Chem. B* **2013**, *1* (38), 4939.

(25) Bakarich, S. E.; Balding, P.; Gorkin, R., III; Spinks, G. M.; in het Panhuis, M. Printed Ionic-Covalent Entanglement Hydrogels from Carrageenan and an Epoxy Amine. *RSC Adv.* **2014**, *4* (72), 38088−38092.

(26) Bai, Y.; Chen, B.; Xiang, F.; Zhou, J.; Wang, H.; Suo, Z. Transparent Hydrogel with Enhanced Water Retention Capacity by Introducing Highly Hydratable Salt. *Appl. Phys. Lett.* **2014**, *105* (15), 151903.

(27) Kirchmajer, D. M.; Gorkin, R., III; in het Panhuis, M. An Overview of the Suitability of Hydrogel-Forming Polymers for Extrusion-Based 3D-Printing. *J. Mater. Chem. B* **2015**, *3* (20), 4105−4117.

(28) Zhou, J.; Ellis, A. V.; Voelcker, N. H. Recent Developments in PDMS Surface Modification for Microfluidic Devices. *Electrophoresis* **2010**, *31* (1), 2−16.

(29) Eddington, D. T.; Puccinelli, J. P.; Beebe, D. J. Thermal Aging and Reduced Hydrophobic Recovery of Polydimethylsiloxane. *Sens. Actuators, B* **2006**, *114* (1), 170−172.

(30) Kim, J.; Chaudhury, M. K.; Owen, M. J.; Orbeck, T. The Mechanisms of Hydrophobic Recovery of Polydimethylsiloxane

DOI: 10.1021/acsami.8b16445
ACS Appl. Mater. Interfaces 2018, 10, 43252−43261

Elastomers Exposed to Partial Electrical Discharges. *J. Colloid Interface Sci.* **2001**, *244* (1), 200−207.
(31) Bodas, D.; Khan-Malek, C. Hydrophilization and Hydrophobic Recovery of PDMS by Oxygen Plasma and Chemical Treatment-An SEM Investigation. *Sens. Actuators, B* **2007**, *123* (1), 368−373.
(32) Vickers, J. A. J.; Caulum, M. M. M.; Henry, C. S. C. Generation of Hydrophilic Poly(Dimethylsiloxane) for High-Performance Microchip Electrophoresis. *Anal. Chem.* **2006**, *78* (21), 7446−7452.
(33) Hegemann, D.; Brunner, H.; Oehr, C. Plasma Treatment of Polymers for Surface and Adhesion Improvement. *Nucl. Instrum. Methods Phys. Res., Sect. B* **2003**, *208* (1−4), 281−286.
(34) Bhattacharya, S.; Datta, A.; Berg, J. M.; Gangopadhyay, S. Studies on Surface Wettability of Poly(Dimethyl) Siloxane (PDMS) and Glass under Oxygen-Plasma Treatment and Correlation with Bond Strength. *J. Microelectromech. Syst.* **2005**, *14* (3), 590−597.
(35) Suni, T.; Henttinen, K.; Suni, I.; Mäkinen, J. Effects of Plasma Activation on Hydrophilic Bonding of Si and SiO[Sub 2]. *J. Electrochem. Soc.* **2002**, *149* (6), G348.
(36) Sharma, V.; Dhayal, M.; Govind; Shivaprasad, S. M.; Jain, S. C. Surface Characterization of Plasma-Treated and PEG-Grafted PDMS for Micro Fluidic Applications. *Vacuum* **2007**, *81* (9), 1094−1100.
(37) Bodas, D.; Khan-Malek, C. Formation of More Stable Hydrophilic Surfaces of PDMS by Plasma and Chemical Treatments. *Microelectron. Eng.* **2006**, *83* (4-9), 1277−1279.
(38) Tóth, A.; Bertóti, I.; Blazsó, M.; Bánhegyi, G.; Bognar, A.; Szaplonczay, P. Oxidative Damage and Recovery of Silicone Rubber Surfaces. I. X-Ray Photoelectron Spectroscopic Study. *J. Appl. Polym. Sci.* **1994**, *52* (9), 1293−1307.
(39) Mata, A.; Fleischman, A. J.; Roy, S. Characterization of Polydimethylsiloxane (PDMS) Properties for Biomedical Micro/Nanosystems. *Biomed. Microdevices* **2005**, *7* (4), 281−293.
(40) Berdichevsky, Y.; Khandurina, J.; Guttman, A.; Lo, Y.-H. UV/Ozone Modification of Poly(Dimethylsiloxane) Microfluidic Channels. *Sens. Actuators, B* **2004**, *97* (2−3), 402−408.
(41) Borcia, C.; Punga, I. L.; Borcia, G. Surface Properties and Hydrophobic Recovery of Polymers Treated by Atmospheric-Pressure Plasma. *Appl. Surf. Sci.* **2014**, *317*, 103−110.
(42) Chen, I.-J.; Lindner, E. The Stability of Radio-Frequency Plasma-Treated Polydimethylsiloxane Surfaces. *Langmuir* **2007**, *23* (6), 3118−3122.
(43) Murakami, T.; Kuroda, S.; Osawa, Z. Dynamics of Polymeric Solid Surfaces Treated with Oxygen Plasma: Effect of Aging Media after Plasma Treatment. *J. Colloid Interface Sci.* **1998**, *202* (1), 37−44.
(44) Awaja, F.; Gilbert, M.; Kelly, G.; Fox, B.; Pigram, P. J. Adhesion of Polymers. *Prog. Polym. Sci.* **2009**, *34* (9), 948−968.
(45) Pressure Sensitive Tape Council. International Standard for Peel Adhesion of Pressure Sensitive Tape. In *Test Methods for Pressure Sensitive Adhesive Tapes*, Oakbrook Terrace, IL, 2012; pp 1−10.
(46) Court, R. S.; Sutcliffe, M. P. F.; Tavakoli, S. M. Ageing of Adhesively Bonded Joints-Fracture and Failure Analysis Using Video Imaging Techniques. *Int. J. Adhes. Adhes.* **2001**, *21* (6), 455−463.
(47) Ollendorf, H.; Schneider, D. A Comparative Study of Adhesion Test Methods for Hard Coatings. *Surf. Coat. Technol.* **1999**, *113* (1−2), 86−102.
(48) Dauskardt, R. H.; Lane, M.; Ma, Q.; Krishna, N. Adhesion and Debonding of Multi-Layer Thin Film Structures. *Eng. Fract. Mech.* **1998**, *61* (1), 141−162.
(49) Lin, Y.; Tsui, T. Y.; Vlassak, J. J. Water Diffusion and Fracture in Organosilicate Glass Film Stacks. *Acta Mater.* **2007**, *55* (7), 2455−2464.
(50) Tang, J.; Li, J.; Vlassak, J. J.; Suo, Z. Adhesion between Highly Stretchable Materials. *Soft Matter* **2016**, *12* (4), 1093−1099.
(51) Leolukman, M.; Kim, S. H. Effect of Rubbing-Induced Polymer Chain Alignment on Adhesion and Friction of Glassy Polystyrene Surfaces. *Langmuir* **2005**, *21* (2), 682−685.
(52) Creton, C.; Ciccotti, M. F. Fracture and Adhesion of Soft Materials : A Review. *Rep. Prog. Phys.* **2016**, *79* (4), 046601.
(53) Fritz, J. L.; Owen, M. J. Hydrophobic Recovery of Plasma-Treated Polydimethylsiloxane. *J. Adhes.* **1995**, *54* (1−4), 33−45.
(54) Tan, S. H.; Nguyen, N. T.; Chua, Y. C.; Kang, T. G. Oxygen Plasma Treatment for Reducing Hydrophobicity of a Sealed Polydimethylsiloxane Microchannel. *Biomicrofluidics* **2010**, *4* (3), 032204.
(55) Maugis, D.; Barquins, M. Fracture Mechanics and the Adherence of Viscoelastic Bodies. *J. Phys. D: Appl. Phys.* **1978**, *11* (14), 1989−2023.
(56) Saffman, P. G.; Taylor, G. The Penetration of a Fluid into a Porous Medium or Hele-Shaw Cell Containing a More Viscous Liquid. *Proc. R. Soc. London, Ser. A* **1958**, *245* (1242), 312−329.
(57) Ghatak, A.; Chaudhury, M. K.; Shenoy, V.; Sharma, A. Meniscus Instability in a Thin Elastic Film. *Phys. Rev. Lett.* **2000**, *85* (20), 4329−4332.
(58) Adda-Bedia, M.; Mahadevan, L. Crack-Front Instability in a Confined Elastic Film. *Proc. R. Soc. London, Ser. A* **2006**, *462* (2075), 3233−3251.
(59) Villey, R.; Creton, C.; Cortet, P.-P.; Dalbe, M.-J.; Jet, T.; Saintyves, B.; Santucci, S.; Vanel, L.; Yarusso, D. J.; Ciccotti, M. Rate-Dependent Elastic Hysteresis during the Peeling of Pressure Sensitive Adhesives. *Soft Matter* **2015**, *11* (17), 3480−3491.
(60) Alvankarian, J.; Majlis, B. Y. Exploiting the Oxygen Inhibitory Effect on UV Curing in Microfabrication: A Modified Lithography Technique. *PLoS One* **2015**, *10* (3), e0119658.
(61) Torres, J. R.; Jay, G. D.; Kim, K.-S.; Bothun, G. D. Adhesion in Hydrogel Contacts. *Proc. R. Soc. London, Ser. A* **2016**, *472* (2189), 20150892.
(62) Brown, W.; Johnsen, R. M. Diffusion in Polyacrylamide Gels. *Polymer* **1981**, *22* (2), 185−189.
(63) Adjari, A.; Brochard-Wyart, F.; de Gennes, P. G.; Leibler, L.; Viovy, J. L.; Rubinstein, M. Slippage of an Entangled Polymer Melt on a Grafted Surface. *Phys. A* **1994**, *204* (1−4), 17−39.
(64) Zhang, B. Separation Strain Rate Dependence on the Failure of Polymer Adhesion with Mobile Promoters. *Int. J. Solids Struct.* **2013**, *50* (25−26), 4349−4354.
(65) Gent, A. N.; Petrich, R. P. Adhesion of Viscoelastic Materials to Rigid Substrates. *Proc. R. Soc. London, Ser. A* **1969**, *310* (1502), 433−448.
(66) Andrews, E. H.; Kinloch, A. J. Mechanics of Adhesive Failure. *Proc. R. Soc. London, Ser. A* **1973**, *332* (1590), 401−414.
(67) Greenwood, J. A.; Johnson, K. L. The Mechanics of Adhesion of Viscoelastic Solids. *Philos. Mag. A* **1981**, *43* (3), 697−711.
(68) Johnston, I. D.; McCluskey, D. K.; Tan, C. K. L.; Tracey, M. C. Mechanical Characterization of Bulk Sylgard 184 for Microfluidics and Microengineering. *J. Micromech. Microeng.* **2014**, *24*, 035017.

DOI: 10.1021/acsami.8b16445
ACS Appl. Mater. Interfaces 2018, 10, 43252−43261